JOURNAL OF MATERIALS SCIENCE **36** (2001) 4267–4272

Hot rolling simulations of austenitic stainless steel

SANG-HYUN CHO
Department of Metallurgical Engineering, McGill University, 3610 University Street, Montreal, Canada H3A 2B2

YEON-CHUL YOO
Department of Materials Science and Engineering, Inha University, 253 Yonghyun-Dong, Nam-Ku, Inchon 402-751, Korea
E-mail: ycyoo@inha.ac.kr

The dynamic, static and metadynamic recrystallization behavior of austenitic stainless steel during hot rolling was analyzed. In this approach, each of those recrystallization behaviors is described by appropriate kinetics equations. The critical strain for dynamic recrystallization was determined so that a distinction could be made between static and metadynamic recrystallization; then the amounts of strain accumulation compared with the critical strain each pass. The effects of grain size on the fraction recrystallized and of the latter on the flow stress were evaluated for each type recrystallization behavior. In this way, the dependence of the mean flow stress (MFS) on temperature could be analyzed in terms of the extent and nature of the prior or concurrent recrystallization mechanisms. Finally, an example is given of an industrial process in which DRX/MDRX can play an important role. More grain refinement can be achieved by increasing the strain rate, decreasing the interruption time and lowering the temperature of deformation.

1. Introduction

Accurate knowledge of the mechanisms acting during hot rolling is important for the manufacture of high quality products, as well as for the design of optimum pass schedules. This in turn requires an understanding of the relationship between hardening and softening during deformation. Many workers have therefore, studied static, dynamic and metadynamic recrystallization behaviors and have developed equations relating their kinetics to the processing parameters [1–6]. Such equations are currently employed in the computer simulation of microstructural evolution during hot working. And, the recrystallization kinetics affect not only the microstructure but also the flow stress. Thus such models can be used to evaluate the effects of modifications to the processing route and can also be employed for on-line process control. Nevertheless, accurate simulation requires the availability of accurate equations.

Hot torsion testing is a powerful tool for studying the hot working behavior of alloys and can be used to provide good physical simulations of actual industrial hot rolling schedules; this is largely because of the large strains that can be attained. The flow stresses and microstructures developed under different simulated rolling conditions have been comprehensively investigated by means of this technique in a series of recent studies [7–9]. Frequently, the effect of changes in the thermomechanical processing variables can't be readily studied by performing industrial mill trials, whereas the laboratory simulation of high strain, multiple-pass hot working processes can be carried out quickly and cheaply, and provide much useful information for optimizing the microstructure, mechanical properties and processing parameters. Nevertheless, in such studies, it is essential to analyze the recrystallization behavior during the entire rolling process very precisely [10].

In this paper, the recrystallization behavior of austenitic stainless steel is characterized under multipass hot rolling conditions. Laboratory simulations were described that have enabled the roles of the various softening mechanisms to be clarified and analyzed.

2. Experimental procedure

AISI 304 stainless steel of nominal composition Fe-18.25 wt% Cr-8.16 wt% Ni was produced by vacuum induction melting and hot rolled as 20 mm thickness. Torsion test specimens with a gauge section of 20 mm length and 5 mm radius were machined from the hot rolled steels. Continuous torsion tests were carried out to determine the critical strain at each experimental temperature and strain rate. Interrupted torsion tests were then conducted over the temperature range 1100–900°C, strain rate range 5.0×10^{-2}–5.0×10^{0}/sec, interpass time range 0.5–100 seconds, and pass strain range 1/4—3 times the peak strain. This was done so

as to evaluate the effects of the deformation variables on metadynamic softening.

The measured torque Γ and twist θ were converted to von Mises effective stress (σ) and strain (ε) using the following equations [11]:

$$\sigma = \frac{3.3\sqrt{3}\Gamma}{2\pi R^3}, \quad \varepsilon = \frac{\theta R}{\sqrt{3}L} \tag{1}$$

Here, R and L are the gauge radius and length of the specimen, respectively. In order to determine the time for 50% recrystallization, the value of the torque associated with yielding was defined using a 0.2% offset method in the multiple twisted torsion tests.

3. Results and discussion

3.1. Dynamic recrystallization

The effect of strain rate on the flow curves of the austenitic stainless steel is shown in Fig. 1. These were determined at a temperature of 1000°C. The peak stress indicating the initiation and occurrence of dynamic recrystallization is clearly seen in all cases and, as expected lower values of peak strain (ε_p) observed at lower strain rates.

This was further confirmed by an analysis of the effect of the deformation conditions on the peak stress (σ_p) using the hyperbolic sine function and the fractional softening attributable to DRX as follows:

$$\dot{\varepsilon} = 2.8 \times 10^{14} (\sinh 0.08\sigma_p)^{5.3} \times \exp(-380000\,\text{J/mol/RT}) \tag{2}$$

$$X_{DRX} = 1 - \exp\left[-0.693\left(\frac{\varepsilon - \varepsilon_c}{\varepsilon_p}\right)^{1.1}\right] \tag{3}$$

and

$$\varepsilon_p = 3.0 \times 10^{-3} D_0^{0.5} Z^{0.09} \tag{4}$$

$$Z = \dot{\varepsilon} \exp(380000\,\text{J/mol/RT}) \tag{5}$$

Here, X_{DRX} is the fractional softening attributable to DRX, ε_c is the critical strain for the initiation of DRX, ε_p is the peak strain and D_0 is the initial grain size.

Strain hardening rate (θ) versus flow stress (σ) curves are shown in Fig. 2 from which the critical strain for DRX can be determined. All the curves meet at a common point identified here as θ_0. Each curve consists of three distinct segments. First, θ decreases linearly with flow stress over a significant portion of the stress-strain curve from θ_0 to the strain at which subgrain formation begins. Second, the θ-σ curve gradually changes to a linear segment of lower slope. Third, the curve drops towards $\theta = 0$ at the peak stress, σ_p. This occurs at the critical stress, σ_c, which identifies the strain at which the DRX becomes operative [12].

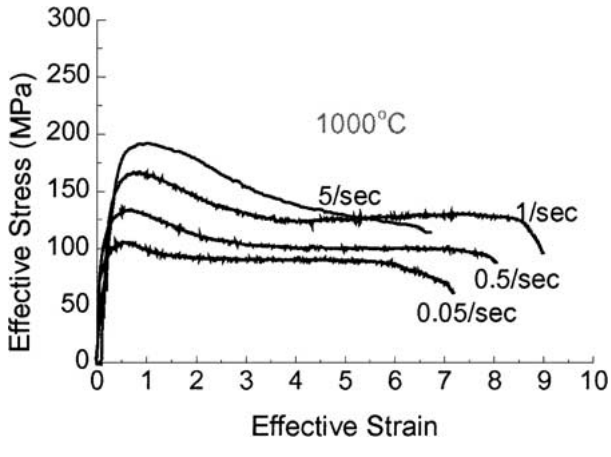

Figure 1 The typical stress-strain curves for austinetic stainless steel.

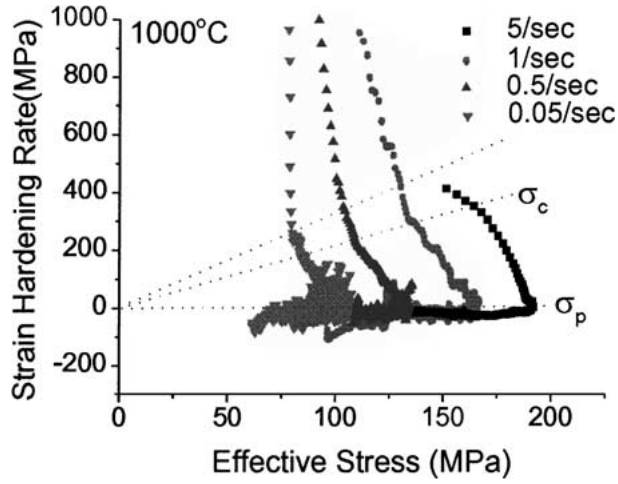

Figure 2 θ-σ curve used to determine the critical strain of 304 stainless steel.

The critical strain can in turn be determined from the original σ-ε curve. In this work, the critical and peak strains as follows: $\varepsilon_c = 0.73\varepsilon_p$; this relationship is in general agreement with literature results ($\varepsilon_c = 0.6$–$0.8\varepsilon_p$) for microalloyed steel [5]. From Fig. 4, the critical strain for DRX can therefore be written as

$$\varepsilon_c = 2.1.0 \times 10^{-3} D_0^{0.5} Z^{0.09} \tag{6}$$

The dependence of the dynamically recrystallized grain size on Zener-Hollomon parameter is illustrated in Fig. 3. To do this, the dependencies of the grain size on temperature and strain rate were obtained. From these results, the grain size can be given by

$$D_{DRX} = 139.5 - 7.3 \log Z \tag{7}$$

The grain size decreased as the Z value was increased in the normal way. As an example, 900°C and 5/sec,

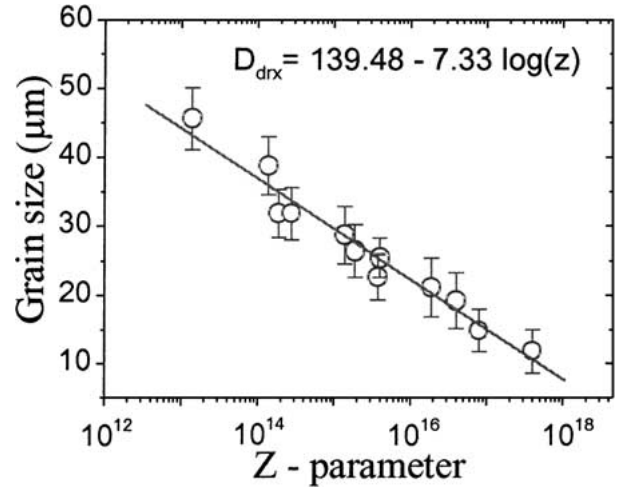

Figure 3 Zener-Hollomon parameter vs. recrystallized grain size for 304 stainless steel.

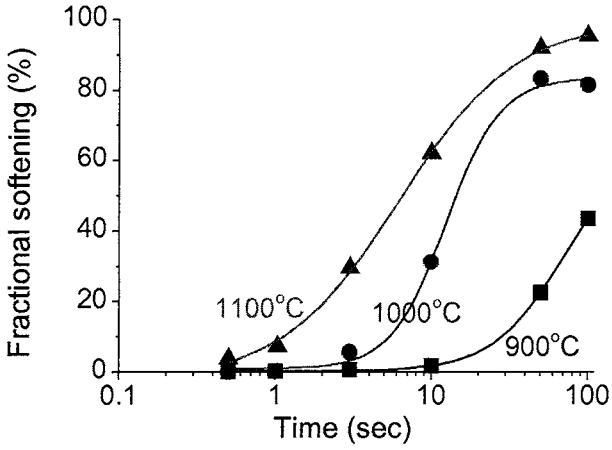

Figure 4 Effect of temperature on the rate of static softening.

the grain size was about 10 μm and a similar value is obtained from the equation.

3.2. Static recrystallization

The static recrystallization kinetics measured as described above are displayed in Fig. 4 for the prior strain rate condition of 0.5/sec and pass strain (ε_i) condition $\varepsilon_i = 0.5\varepsilon_p$. These strains were determined from Equation 4 to be well below the critical strain for the initiation of DRX. Thus, the softening kinetics determined were for SRX. All the softening curves display the typical sigmoidal shape and the recrystallization kinetics can be described by the usual Avrami equation:

$$X_{SRX} = 1 - \exp\left[-0.693\left(\frac{t}{t_{50\text{ for SRX}}}\right)^{1.02}\right] \quad (8)$$

Here

$$t_{50\text{ for SRX}} = 2.0 \times 10^{-10}\dot{\varepsilon}^{-0.8}\varepsilon^{-1.6}D_0 \times \exp(197000\,\text{J/mol/RT}) \quad (9)$$

The Avrami time exponent of 1.02 and the exponents of -0.8 and -1.6 strain rate and strain were determined by considering the effect of each variable on the softening kinetics respectively. Many researchers have reported Avrami time constant values was 1–2 for carbon and microalloyed steels; they are also in good agreement with earlier results on austenitic stainless steel [6, 13, 14].

All investigations of SRX kinetics reveal a weak effect of strain rate, but a strong effect of pass strain and initial grain size. Since the driving force for SRX is the reduction of strain energy by annihilation of the dislocations introduced during deformation, the significant influence of strain is to be expected.

If softening takes place by SRX and there is sufficient time for recrystallization to proceed, the grain size is given by

$$D_{SRX} = 8.6\,\varepsilon^{0.4}D_0^{0.5}t_i^{-0.2}Z^{-0.05} \quad (10)$$

here, ε is the pass strain, D_0 is initial grain size and t_i is the interruption time. The relationship between statically recrystallized grain size and pass strain could be expressed by the following power relation; $D_{SRX} \propto \varepsilon^{0.4}$. Also, the dependencies of statically recrystallized grain size on temperature, strain rate, interruption time and initial grain size were obtained by the above method.

In conventional SRX, the final grain size depends sensitively on the initial grain size and the pass strain but is not particularly affected by the temperature. This reflects the significant influence of the initial microstructure on the number of nuclei, which is the characteristic that essentially controls the recrystallized grain size.

3.3. Metadynamic recrystallization

The effect of temperature on the kinetics of postdynamic or metadynamic recrystallization is displayed in Fig. 5a. Dynamic recrystallization was induced in this material by deforming it to the peak strain at strain rate of 0.5/sec. Here, the behavior illustrated is typical in that it can again be modeled using Avrami kinetics, in which the metadynamically recrystallized fraction is given by

$$X_{MDRX} = 1 - \exp\left[-0.639\left(\frac{t}{t_{50\text{ for MDRX}}}\right)^{1.06}\right] \quad (11)$$

where

$$t_{50\text{ for MDRX}} = 1.3 \times 10^{-11}\dot{\varepsilon}^{-0.4}D_0 \times \exp(230000\,\text{J/mol/RT}) \quad (12)$$

In this work, the curves for $\dot{\varepsilon} = 5$, 0.5 and 0.05/sec were regularly spaced, (see Fig. 5b) and the corresponding strain rate exponent, n, for the time to 50% softening (Equation 12) is found to be 0.4. This compares with

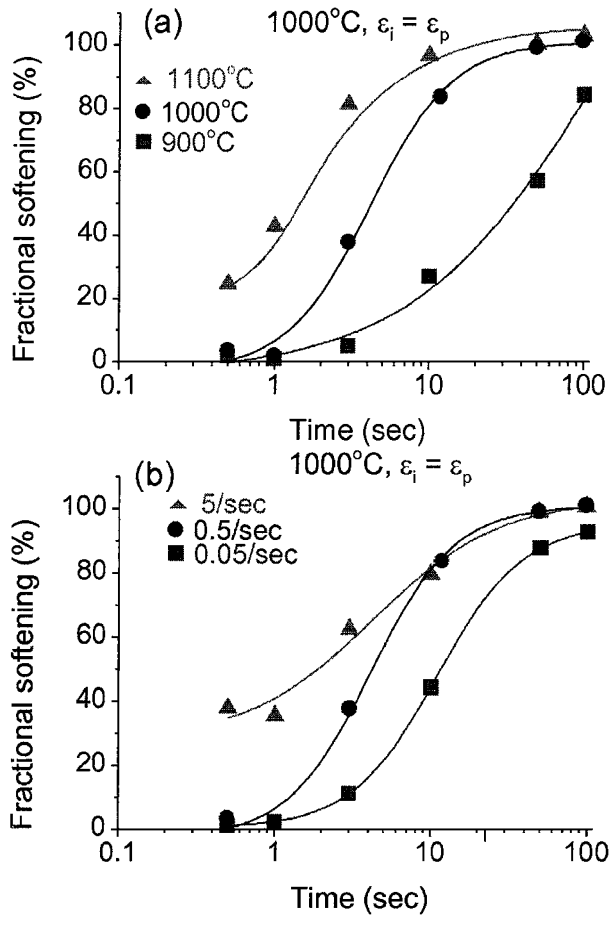

Figure 5 Effect of temperature (a) and strain rate (b) on the rate of metadynamic softening.

values of $n = 0.8$ reported by Hodgson *et al*. and $n = 0.6$ determined by Roucoules *et al*. for HSLA steel [13, 15].

In the case of SRX kinetics, most investigations have revealed a weak effect of strain rate but a strong effect of pass strain. Since the driving force for SRX is the reduction in strain energy, basically annihilation of the dislocations introduced during deformation, a significant influence of strain is to be expected. In the case of MDRX, the driving force is same but the dislocation density is that produced by DRX. Once the pass strain is exceeds the critical strain for DRX, changes in the pass strain do not affect the dislocation density to away significant extent. The MDRX kinetics are not, therefore, expected to be affected by increases in strain.

If there is softening by MDRX, and therefore sufficient time for this type of recrystallization to proceed, the subsequent grain size is given by

$$D_{\mathrm{MDRX}} = 6.1 D_0^{0.5} t_{\mathrm{i}}^{-0.17} Z^{-0.06} \tag{13}$$

here, D_0 is initial grain size. This relationship between metadynamically recrystallized grain size and deformation variables was obtained by the above method which is Equation 10.

Although SRX during the interpass intervals is relatively slow during hot rolling, the same statement does not apply to MDRX. This type of softening is considerably more rapid than SRX, so that some grain coarsening generally occurs during cooling after deformation once straining has been extended into the dynamic recrystallization regime.

When recrystallization by MDRX or SRX is only partial, some strain is retained into the next pass. Under these conditions the accumulated strain (ε_{a}) can be calculated from the following relation [15]:

$$\varepsilon_{\mathrm{a}} = \varepsilon_{\mathrm{i}} + (1 - X_{\mathrm{i}-1})\varepsilon_{\mathrm{a}-1} \tag{14}$$

This is the strain value that is inserted into Equation 6 to determine whether DRX (followed by MDRX) is initiated during that pass or not. If the calculated accumulated strain is greater than the critical strain for DRX, X represents the MDRX fraction; if not X stands for the SRX fraction.

3.4. Hot rolling simulation and analysis

The hot rolling process that was simulated in these experiments is illustrated in Fig. 6. Here, the temperature decreases from 1100 to 900°C, the interruption time decreases from 10 to 1 second, the pass strain decreases from 40 to 10% and the strain rate increases from 0.05 to 5/sec. The set of strainstress curves obtained when this simulation was carried out on the torsion machine is shown in Fig. 7.

Here, the specimen was cooled at about 3°C/sec and the strain rate was increased after each cycle of deformation. It can be seen that the stress level in each pass increases gradually, due to the continuous decrease in temperature and increase in strain rate. After about 6th pass, the rate of flow stress change increases sharply. This is because strain accumulation, i.e., the retention of work hardening, is beginning to take place as the sample temperature is now below the no-recrystallization temperature, T_{nr} [16, 17].

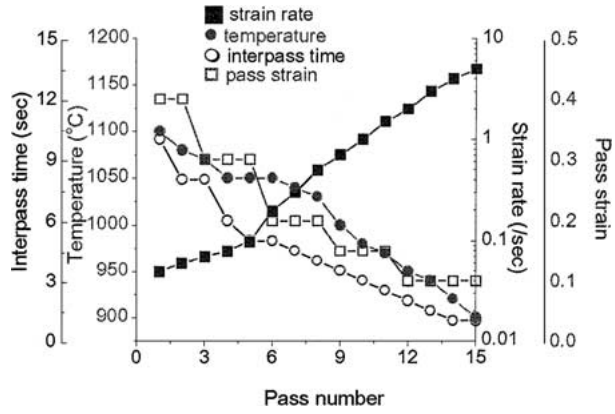

Figure 6 Simulated multistage hot rolling process schedule.

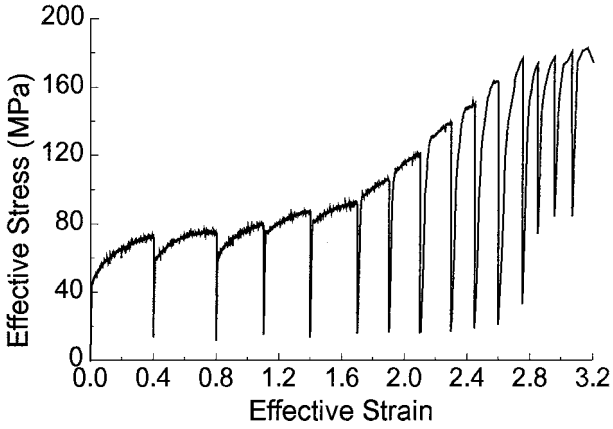

Figure 7 Stress-strain curve for the simulation of Fig. 7's schedule.

The flow chart describing the hot rolling simulation procedure is displayed in Fig. 8. When dynamic recrystallization is taking place, Equations 2–7 are used to calculate the critical strain, peak strain and grain size. Equations 8–13 are used to predict the kinetics of SRX/MDRX, the amount of strain accumulation, the grain size, etc.

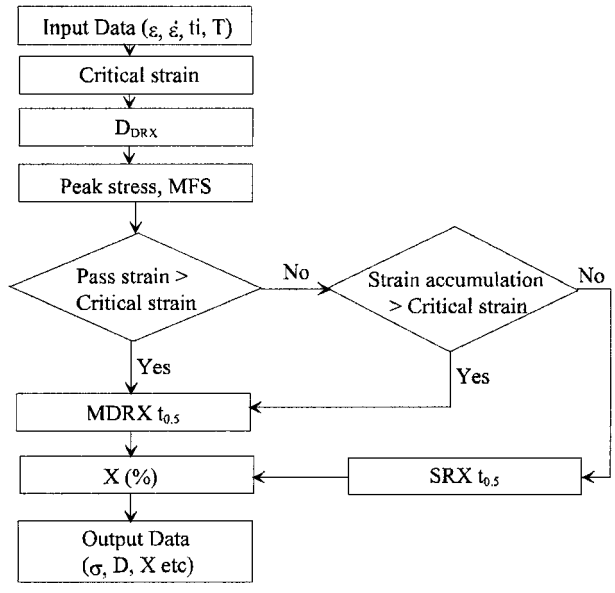

Figure 8 Outline of a prediction procedure for simulated hot rolling process.

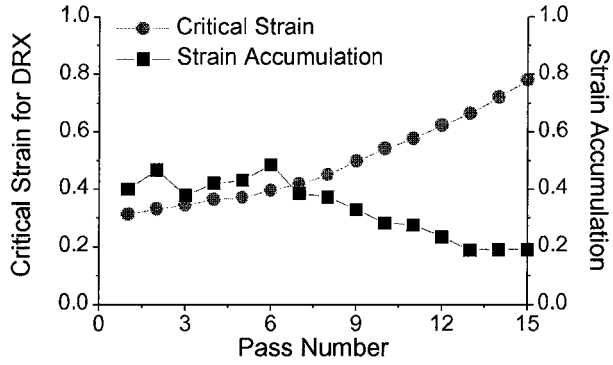

Figure 9 The comparison between critical strain for DRX and strain accumulation to determine the transition of MDRX/SRX.

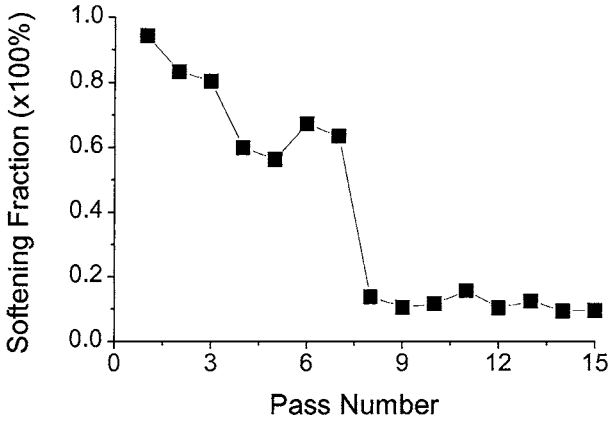

Figure 10 Calculated fraction softening according to recrystallization behavior.

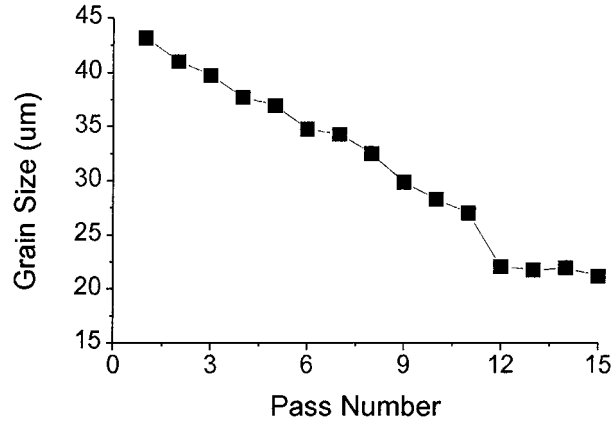

Figure 11 Grain size prediction for simulated hot rolling process.

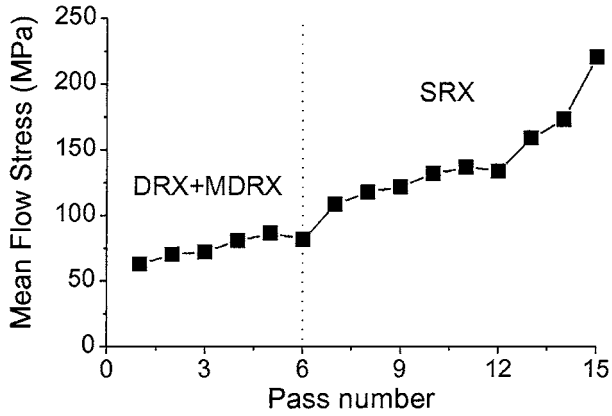

Figure 12 Mean flow stress for simulated process, showing DRX evidence in early passes, followed by MDRX.

The critical strain for DRX calculated from Equation 6 and the strain accumulation obtained from Equation 14 are compared in Fig. 9. As the pass number is increased, the pass strain decreases, as shown in Fig. 6; the strain accumulation decreases and the critical strain is less than accumulation after the 7th pass. This shows that DRX/MDRX leads the kinetics, microstructure changes and rolling loads within the 7th pass.

The amounts of softening taking place between passes as; determined from Equations 8 and 11, are illustrated in Fig. 10. According to Fig. 9, which defines the boundary between MDRX and SRX, the softening behavior can be divided into two regions: MDRX is dominant until the seventh pass, after words, these is recovery, but no SRX. The fractional softening by MDRX is higher than that produced by SRX in the early stages. This is because MDRX does not require an incubation time.

Fig. 11 displays the grain size in each pass called for by Equations 7, 10, and 13. In the case of SRX, the grain size depends on all deformation variables like $\dot{\varepsilon}$, t_i, ε_i, T etc. The same principle holds for the grain size after DRX, but since the DRX structure is controlled only by Z (Z contains only $\dot{\varepsilon}$ and T), it follows that the DRX grain size and hence the MDRX grain size are also functions of the Z value.

Furthermore, the MDRX kinetics is more fast than that of SRX during interruption time. Therefore, in Fig. 11, it can be found that the grain size is decreased linearly up to the end of MDRX and then, there is just little slope change. The final grain size was observed to be 25 μm, but the predicted by Equations 7, 10, and 13 grain size was 21 μm. This difference may be attributed to grain growth during cooling. As shown in the rolling schedule, the final testing temperature was 900°C and the specimen was air cooled cooling after rolling. Therefore, it's enough to grow the grain.

The mean flow stresses (MFS) generated during the hot rolling simulation are displayed as a function of pass number in Fig. 12. The mean flow stress (MFS) is calculated as the area under a given stress-strain curve for the strain interval selected in this experiments. Therefore, the MFS between strains ε_1 and ε_2 is calculated as follows:

$$\text{MFS} = \frac{1}{(\varepsilon_2 - \varepsilon_1)} \int_{\varepsilon_1}^{\varepsilon_2} \sigma \, \mathrm{d}\varepsilon \qquad (15)$$

The contrasting pass number dependencies of DRX followed by MDRX, some SRX and strain accumulation can be seen in this diagram. When DRX followed by MDRX takes place, the rate of increase of MFS is relatively low and drops away from that associated with large pass strain ($\varepsilon_i > \varepsilon_c$) in the early stage. When some SRX takes place, the rate of increase of MFS is also low, but when strain accumulation is occurring (i.e. at temperature below the T_{nr}), there is sharp increase in slope. Then, it can be expected easily to decrease the rate of

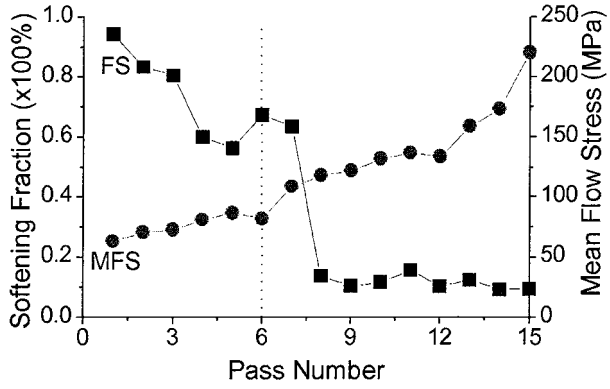

Figure 13 The comparison between fractional softening and mean flow stress.

MFS after strain accumulation, because the accumulation of retained work hardening leading to the initiation of DRX. When DRX is initiated, followed by MDRX, the rate of flow stress increase drops and also, related with grain refinement.

Therefore, it is important that DRX can take place in practical hot rolling process, especially for high speed tandem mill like strip or rod mill. The common factor in these processes is relatively very short interruption time. If these times are fully enough to restrict SRX, then enough strain can be accumulated, in a series of successive pass, to trigger the DRX. However, it can not be found that the T_{nr}. It's because there is no strong carbide former elements like Nb, V and Ti etc. in austenitic stainless steel

The mean flow stress (MFS) is normally the most important factor affecting the rolling force during finish rolling [16, 17]. In addition to strain accumulation, it is also influenced by the microstructural events that take place, such as SRX, DRX and MDRX. DRX and MDRX affect the rolling force and grain size through the removal of dislocations and work hardening. The evolution of microstructure that takes place during rolling also modifies the final properties of the steel. It is, therefore important to know whether or not DRX and MDRX occur during multipass deformation.

One interesting result is displayed in Fig. 13. In Fig. 13, the MFS and fractional softening are compared. This figure indicates that the value of softening, which changes the softening behavior decreases rapidly and the point correspond to the result obtained from MFS slope. It is important to note that the transition point of recrystallization behavior can be also determined by recrystallization kinetics.

4. Conclusions

The kinetics equations of recrystallization behaviors during hot deformation was described and changes in softening was analyzed in the simulated hot rolling process. From the analysis of softening behavior, the following conclusions can be drawn:

1. The modeling equations, which can explain softening behavior during hot deformation can be suggested.
2. The initiation of DRX during multipass deformation leads to change the recrystallization behavior during simulated rolling process.
3. The DRX/MDRX softening kinetics is faster than that of SRX and with grain refinement, DRX and MDRX can result in fine grain size.
4. The pass to pass softening can also be confirmed by calculating the mean flow stress (MFS). The slope of MFS is low in the DRX/MDRX region and increases gradually in the SRX regions and finally increases sharply due to the strain accumulation.

Acknowledgments

The authors gratefully acknowledge the financial support of the Korean Science and Engineering Foundation.

References

1. C. M. SELLARS and J. A. WHITEMAN, *Mat. Sci.* **13** (1979) 187.
2. B. DUTTA and C. M. SELLARS, *Mater. Sci. Technol.* **3** (1987) 197.
3. C. M. SELLARS, in Proc. Int. Conf. on HSLA Steela '85, edited by J. M. Gray *et al.* (Am. Soc. Met. Metals Park, USA, 1986), p. 73.
4. P. D. HODGSON and R. K. GIBBS, *ISIJ Int.* **33** (1993) 1257.
5. P. CHOQUET, P. FABREGURE, J. GIUSTI, B. CHAMONT, J. N. PENSANT and F. BLANCHET, in Proc. Int. Symp. Mathematical Modeling of Steel, Hamilton, Canada, edited by S. Yue (Can. Inst. Mining & Metallurgy, 1990), p. 232.
6. O. KWON, *ISIJ Int.* **32** (1992) 350.
7. E. A. SIMIELLI, S. YUE and J. J. JONAS, *Metal. Mater. Trans. A* **23A** (1992) 597.
8. J. W. BOWDEN, F. H. SAMUEL and J. J. JONAS, *ibid.* **22A** (1991) 2947.
9. L. N. PUSSEGODA, S. YUE and J. J. JONAS, *ibid.* **26A**(1) (1995) 181.
10. T. M. MACCAGNO and J. J. JONAS, *ISIJ Int.* **34** (1994) 607.
11. S. L. SEMIATIN, G. D. LAHOTI and J. J. JONAS, "ASM Metals Handbook," 9th ed. Vol. 8 (American Soc. Mater., Metals Park, USA, 1985) p. 154.
12. L. N. PUSSEGODA, S. YUE and J. J. JONAS, *Metall. Trans. A* **21A** (1990) 153.
13. C. ROUCOULES, P. D. HODGSON, S. YUE and J. J. JONAS, *ibid.* **25A** (1994) 389.
14. LAASRAOUI and J. J. JONAS, *Metall. Trans.* **22A** (1991) 151.
15. P. H. HODGSON and R. K. GIBBS, *ISIJ Int.* **32** (1992) 365.
16. L. P. KARJALAINEN, T. M. MACCAGNO and J. J. JONAS, *ibid.* **35** (1995) 1523.
17. S. H. CHO, S. I. KIM and Y. C. YOO, *J. Mater. Sci. Lett.* **16** (1997) 1836.

Received 15 February 2000
and accepted 13 April 2001